Iraqi Journal of Science, 2024, Vol. 65, No. 10(SI), pp: 6070- 6078
DOI: 10.24996/ijs.2024.65. 10(SI).14

ISSN: 0067-2904

Atmospheric Turbulence Parameters Deduced from Vertical Profile of Cn_2

Raaid Nawfee Hassan
Department of Astronomy and Space, College of sciences, University of Baghdad, Baghdad, Iraq.

Received: 5/10/2023 Accepted:26/6/2024 Published: 15/11/2024

Abstract

The proposed framework can capture realistic spatiotemporal variations in atmospheric turbulence parameters based on local meteorological conditions, such as Fried's parameter r_0, isoplanatic angles θ_0, seeing ε, scintillation rate δ_I^2, and the wavefront coherence time τ_0. Those parameters have been deduced from the refractive index structure parameter C_n^2 Two Iraqi locations were compared, specifically the middle and southern borders, and atmospheric turbulence parameters relevant to astronomical observation were measured, lines were drawn at latitudes 34.26° and 28.31°, respectively. The methodology included collecting meteorological data from both sites and performing numerical simulations based on atmospheric turbulence parameters. According to the criteria of air turbulence, the results showed that the middle of Iraq was better than the southern location for astronomical observation.

Keywords: Refractive structure constant, coherence time, Fried's parameter, optical turbulence, applied optics.

عناصر الاضطراب الجوي المستخلصة من الملف العمودي لـCn2

رائد نوفي حسان

قسم الفلك والفضاء، كلية العلوم، جامعة بغداد، بغداد، العراق

الخلاصة

يمكن للإطار المقترح التقاط الاختلافات الزمانية المكانية الواقعية في عناصر الاضطراب الجوي بناءً على ظروف الأرصاد الجوية المحلية، مثل عامل فريد r_0 ، والزوايا المسطحة θ_0 ، وظروف الرؤية ε ، ومعدل التلألؤ σ_I^2 ، وزمن تشاكه واجهة الموجة τ_0 . و قد تم استنتاج هذه المعلمات من معلمة بنية معامل الانكسار C_n^2 . وتمت مقارنة موقعين عراقيين، وتحديداً الحدود الوسطى والجنوبية، وتم قياس بارامترات الاضطراب الجوي ذات الصلة بالرصد الفلكي، ورسمت الخطوط عند خطي عرض 34.26° و 28.31° على التوالي . وتضمنت المنهجية جمع بيانات الأرصاد الجوية من كلا الموقعين وإجراء عمليات محاكاة رقمية بناءً على معلمات الاضطرابات الجوية . وبحسب معايير الاضطراب الجوي أظهرت النتائج أن وسط العراق أفضل من الموقع الجنوبي للرصد الفلكي .

*Email: raaid.hassan@sc.uobaghdad.edu.iq

1. Introduction

Optical turbulence refers to the variations in the refraction index with atmospheric turbulence as their origin. A significant problem for ground-based astronomy is the limiting resolution of an image that has been imposed by atmospheric turbulence, besides the limit that an optical instrument has imposed [1]. The large diameter of the new telescopes increases the amount of light collected by the instrument; however, it cannot help in obtaining a higher spatial resolution in an image [2]. Atmospheric turbulence changes the phase and amplitude of incoming wavefronts and images in a stochastic manner [3]. The refractive index structure parameter C_n^2 ($m^{-2/3}$) is used to quantify the strength of optical turbulence. This quantity can be thought of as how strong the refractive index fluctuations are, and it is physically defined at every instant and in every position [4]. The effects of atmospheric turbulence cannot be eliminated, even with long or large telescopes. In general, atmospheric turbulence is the root cause of degradation in astronomical image quality and resolution[5].

Various parameters have been utilized to characterize the intensity of turbulence in the atmosphere: Fried's parameter r_0, isoplanatic angles θ_0, seeing ε, rate of scintillation σ_I^2, and wave-front coherence time τ_0. Every one of those parameters has relevance for specific astronomical applications [6]. The study aimed to compare two locations in Iraq, specifically the middle and southern borders for measuring atmospheric turbulence parameters relevant to astronomical observation. The results support the suitability of the middle border of Iraq for such observations, and provide insights for site testing, improving adaptive optics approaches, and scheduling flexibility in astronomical research.

The aim of the study was to compare the two regions of Iraq, the middle and southern borders, in term of atmospheric turbulence parameters that have strong impact on astronomical observations. The results obtain a site testing, adaptive optics approaches, and scheduling flexibility in astronomy research.

2. Integrated Astro-climatic Parameters

Understanding atmospheric optical quality is essential for various applications, particularly an adaptive optics field (AO), where parameters like seeing C_n^2 ,ε and length of coherence r_0 play a crucial role. These parameters depend on local conditions at a specific altitude value. In AO systems, seeing ε serves as a key parameter for identifying optimal observation windows for r_0 retrieval [7]. The coherence time τ_0 is determined based on wind speed and profiles [8]. To provide reference values for astronomical observations, it is imperative to accurately calculate and present these parameters [9]. In this study, we use the point light mode approach to analyze and present the relevant atmospheric parameters:

$$r_0 = \left[0.423\left(\frac{2\pi}{\lambda}\right)^2 \int_0^\infty C_n^2(h)dh\right]^{-3/5} \quad \ldots\ldots\ldots(1)$$

$$\varepsilon = 5.25\lambda^{-1/5}\left[\int_0^\infty C_n^2(h)dh\right]^{3/5} \quad \ldots\ldots\ldots(2)$$

$$\tau_o = 0.057\lambda^{6/5}\left[\int_0^\infty |V(h)|^{5/3} C_n^2(h)dh\right]^{-3/5} \quad \ldots\ldots\ldots(3)$$

The scintillation rate has been represented as follows [10]:

$$\delta_I^2 = 19.12\lambda^{6/5} \int_0^{\infty} h^{5/3} C_n^2(h) dh \quad \ldots\ldots\ldots (4)$$

Isoplanatic angle θ_0 has been characterized as the maximal angular separation of two stellar objects that produce similar wave-fronts at the telescope entrance pupil, can be expressed by the analytical expression [2][11]:

$$\theta_0 = 0.057\lambda^{6/5} \left[\int_0^{\infty} h^{5/3} C_n^2(h) dh \right]^{-3/5} \ldots \quad \ldots\ldots (5)$$

Astro-climate imposes constraints on astronomical observations [12]. The turbulent fluctuations in the refractive index of air at various heights affect the electromagnetic wave that propagates in the atmosphere of the Earth [13]. Therefore, the results of the turbulence in the image's motion and the fluctuations of the spatial intensity (i.e., the scintillations) in the astronomical telescope focus on the turbulence in the atmosphere of the Earth and represents a complex phenomenon that covers a wide variety of temporal and spatial scales [14]. In the electromagnetic spectrum's optical range, turbulence fluctuations in the refractive index of air are proportional to temperature fluctuations and undergo turbulent air motions. The crucial atmospheric turbulence parameter defining the resolving power of a telescope is the constant of the structure of the refractive index, which is represented C_n^2 based on the Kolmogorov model, C_n^2 which represents the energy of the small-scale 3-D homogeneous isotropic turbulence spectrum. The quantity C_n^2 is related to the structure constants of their temperature C_T^2 or the speed of the wind C_V^2 [15].

Understanding the height profile represents the basis for describing the variations in statistical features of the quality of an image in a turbulent atmosphere [16]. For instance, the atmospheric resolving power of the telescope β can be expressed by the following equation [17]:

$$\beta = \frac{0.98\lambda}{(0.423k^2 sec\ \alpha \int_0^H C_n^2(h) dh)^{-3/5}} \quad \ldots\ldots\ldots (6)$$

Where λ denotes wavelength, $k = 2\pi/\lambda$, h denotes height, α denotes zenith angle, and h denotes the upper boundary of the optically active atmosphere (~35km) scales. Many researchers have described a vertical dependence of the parameter of the refractive index structure [18], with one of the most commonly used being the Hufnagel–Valley model [19]:

$$C_n^2 = 8.2 * 10^{-26} h^{10} e^{-h} W^2 + 2.7 * 10^{-16} e^{-\frac{h}{1.5}} + A e^{-h/0.1} \quad \ldots\ldots\ldots (7)$$

Here, h denotes height above ground (kilometers), W^2 denotes the square average of the wind speed at an altitude of (5–20) km, and A is a constant.

3. Observational Data Description

The observational data from the University of Wyoming Atmospheric Science Radiosonde Archive (UWASRA) was used [20]. The stations' information and sounding indices for the two locations are are presented in Table 1:

Table 1 : Station information

Observational Data	First Location	Second Location
Station identifier	OICC	OEPA
Station No.	40766	40373
Observation time	2022/11/28	2022/11/28
Station latitude	34.26	28.31
Station elevation	1322.0	358.0
Station longitude	47.11	*46.13*
Pressure [hPa] of the Lifted Condensation Level	769.33	762.16
Temp. [K] of Lifted Condensation Level	272.16	274.83
Equivalent potential temp. [K] of LCL	307.12	314.02
Average mixed layer potential Temperature	293.36	297.03

4. Results and Discussion

The present work compares two locations for measuring the atmospheric turbulence parameters in the following sections.

4.1. Metrological Comparison

The metrological data (relative humidity, temperature, pressure, wind speed, and wind direction) used in the comparison were obtained from two stations with observation times of 11/28/2022 for two locations in Iraq's middle and south borders (47.11^{o}E, 34.26^{o}N) and (46.13^{o}E, 28.31^{o}N). According to the criteria of air turbulence for testing the best position for astronomical observation. It is especially notable that, despite being separated by 6^{o}N latitude and 964 m elevation, the observational results of the two sites were similar behavior. As seen in Figure 1, the peak relative humidity was observable in the height range of 7–14 km for two stations. Also, in this figure for wind direction variation, two peaks are observable at 1 km and 22 km, respectively, but the secondary peak for the lower latitude (28.31^{o}N) is much stronger than that for the upper latitude (34.26^{o}N).

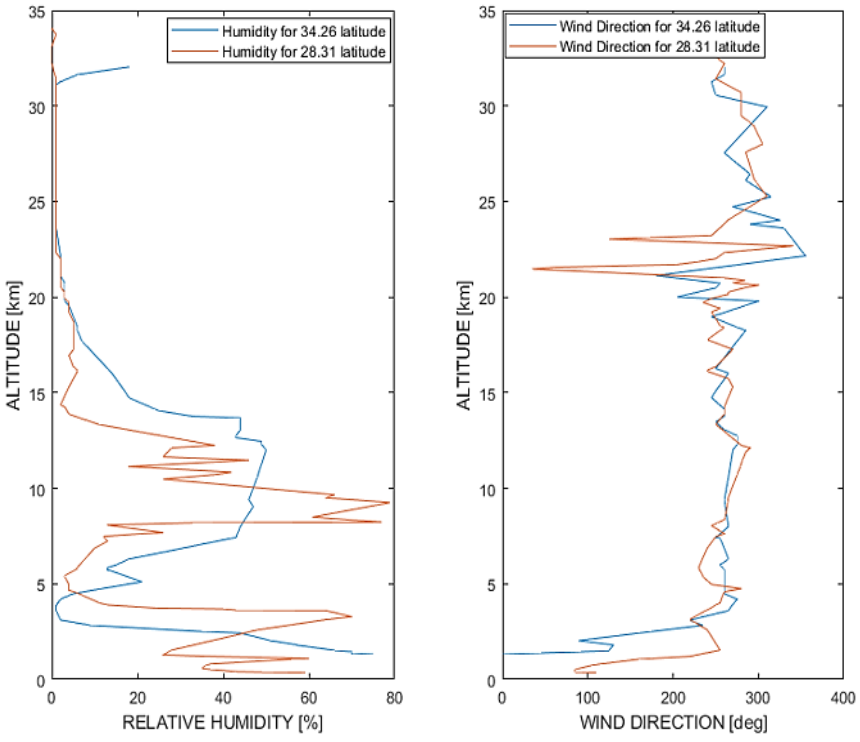

Figure 1: Vertical profile of the relative humidity and wind direction.

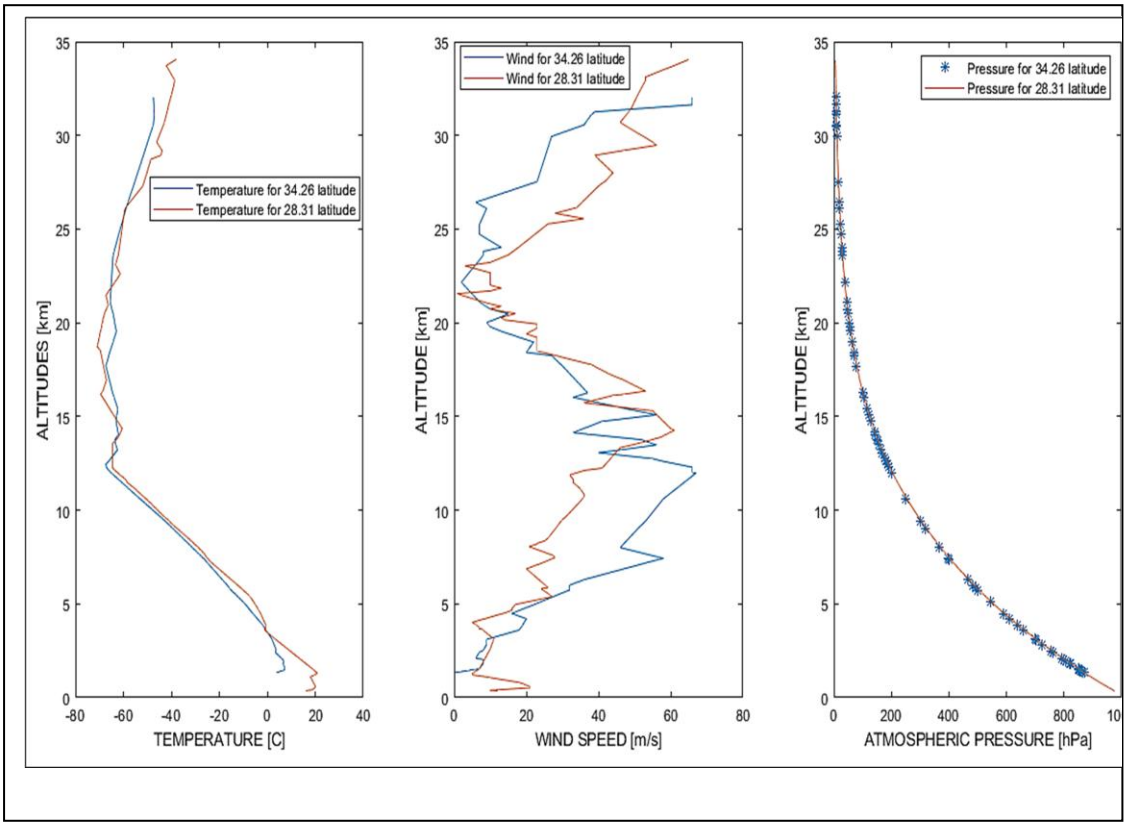

Figure 2 : Vertical profile of the temperature, wind speed, and

It can be seen that the atmospheric pressure gradually decreased (Figure 2). During the high consistency in the variability of the meteorological factors (e.g., temperature, wind speed, and pressure) vs. height.

In Figure 3, the first two curves show the identical calculation of C_n^2 using the Hufnagel–Valley model for two locations as a function of altitude and wind speed, respectively. The third curve represents the atmospheric pressure as a function of wind speed in two distinct regions, the first when the wind speed decreases (about 1 m/s) and the second when the wind speed increases (60 m/s), with a reversal relationship. From Figure 3, through careful observation, the difference in the overall data can be found, especially when taking it C_n^2 as a function of altitude, the strong turbulence near-surface (0 – 5 km) level, and below 15 km in the troposphere, consistent with the two locations that was selected.

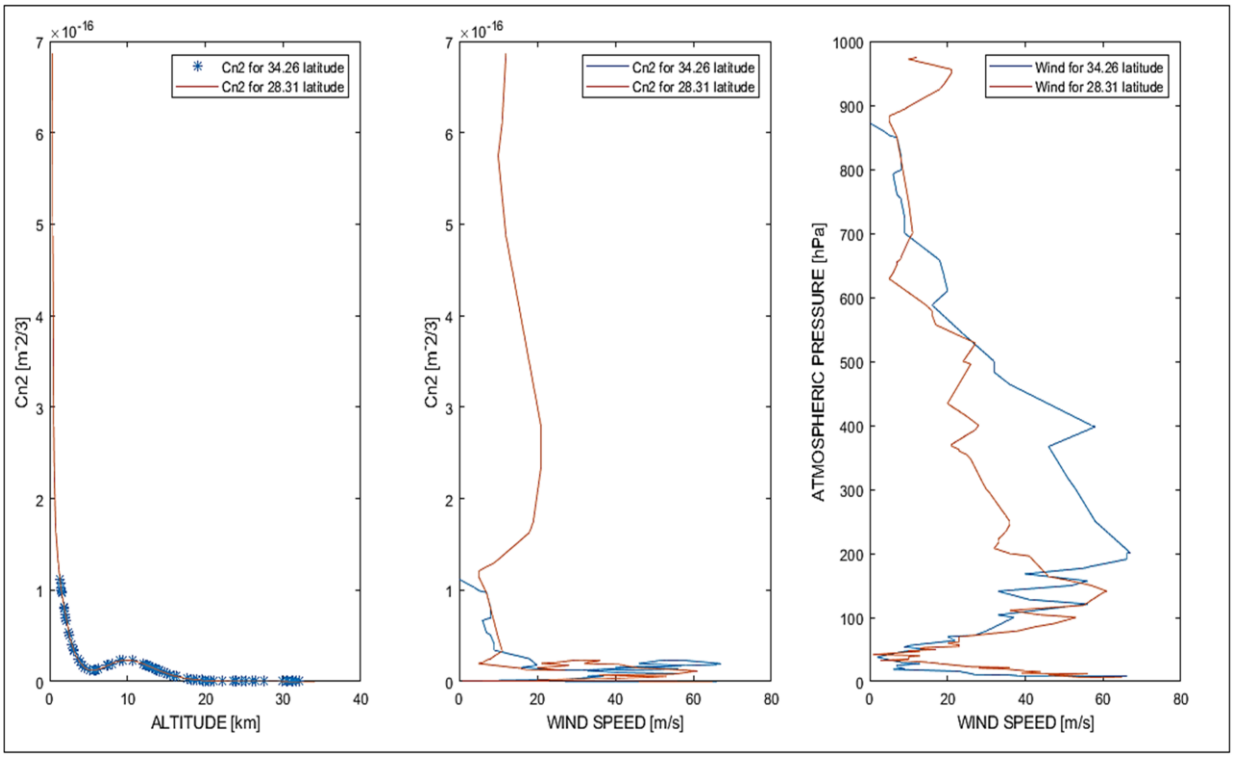

Figure 3:From left to right: The profile of the constant of the refractive index structure as a function of altitude and wind speed, the last one represents pressure vs. wind speed.

4.2. Astro-climatic Parameters of Air Turbulence Comparison

The Astro-climatic Parameters: Fried's parameter r_0, seeing ε, isoplanatic angles θ_0, and scintillation rate σ_I^2 were compared for two stations with an observation time of Nov 28, 2022. Figures (4-8) show the criteria for air turbulence (r_0, σ_I^2, ε, θ_0, τ_0) as a wind speed function for two site selections.

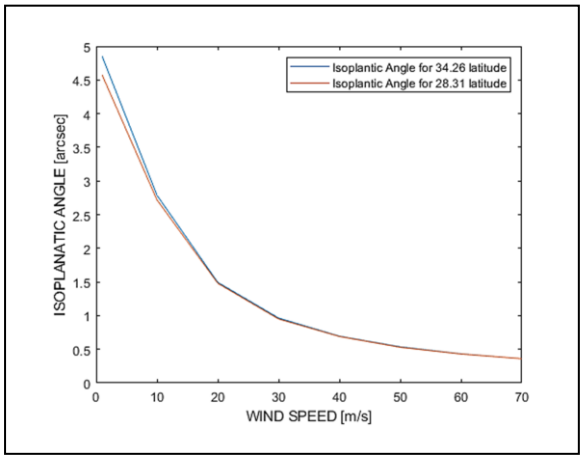

Figure 4: The inversion relationship between isoplanatic angle parameter and wind speed

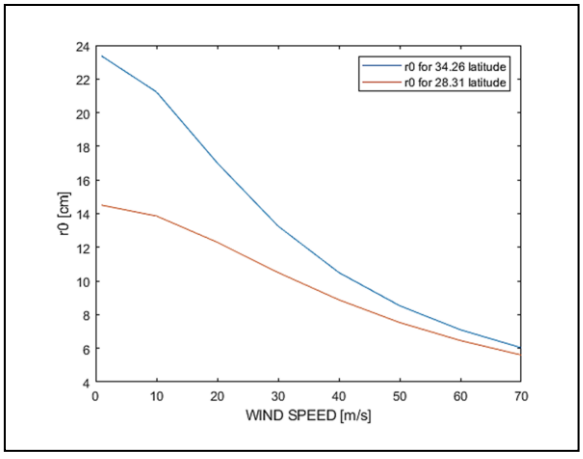

Figure 5:The inversion relationship between Fried's parameter and wind speed

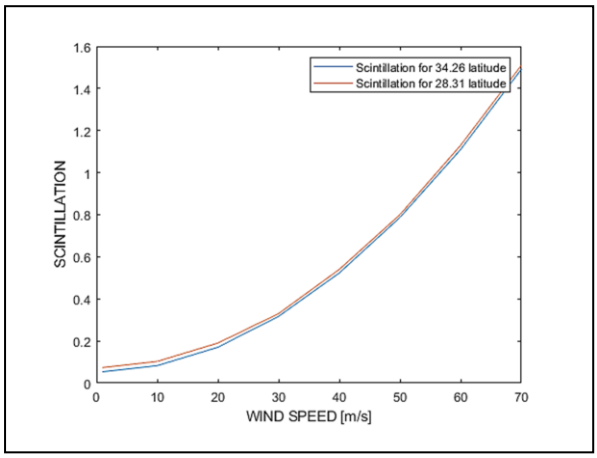

Figure 6: The preoperational relationship between scintillation parameter and wind speed

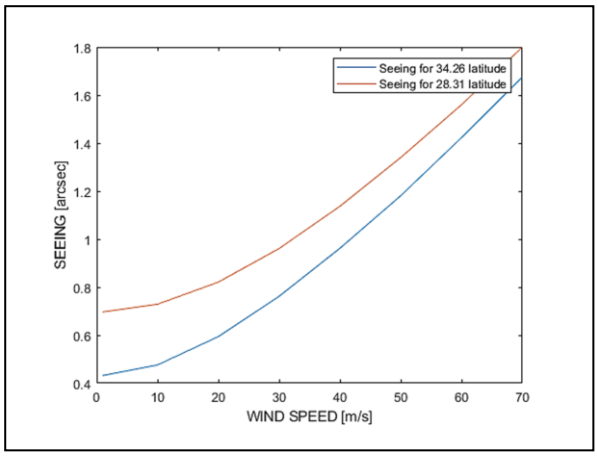

Figure 7: The preoperational relationship between seeing parameter and wind speed

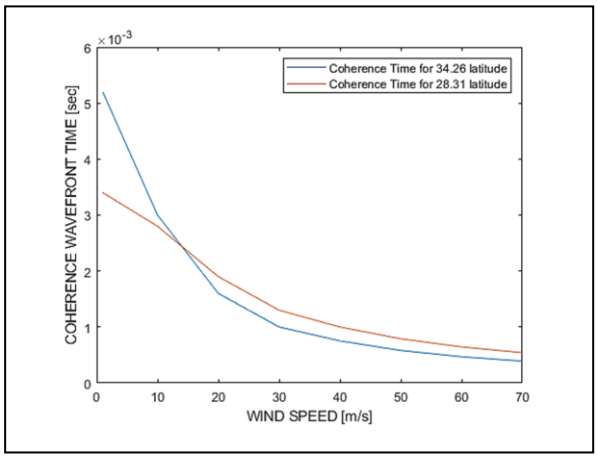

Figure 8: The inversion relationship between coherence time parameter and wind speed

All figures above and according to the criteria of air turbulence, it could be found that the best location for astronomical observation was the middle border of Iraq. This is because of the presence of the Shatt Al-Arab Gulf in southern Iraq, which causes the most significant amount of turbulence. Poor seeing values identify the area around the gulf, and finally, a more significant seeing has been discovered beside the higher longitude area, away from rivers, and above sea level (higher elevation).

Conclusions

This paper describes the general characteristics of a meteorological model, the model's parameters that characterize optical turbulence, and the potential applications of this tool for site testing, optimizing adaptive optics approaches, and enhancing scheduling flexibility. The model has been shown to be sensitive to geographic effects, and the impact of horizontal and vertical location on simulation output was tested. The procedure was supported by comparing two stations on Iraq's middle and southern borders. Atmospheric turbulence parameters were compared based on local meteorological conditions, such as Fried's parameter (r_0), seeing (ε), isoplanatic angle (θ_0), scintillation rate (σ_I^2), and wavefront coherence time ($\boldsymbol{\tau}_0$). According to

the results, the middle border of Iraq proved to be better for observation than the southern border.

References

[1] R. H. Foadi, and A. K. Ahmed, "Designing Cassegrain Telescope System with Best Obscuration Ratio of Secondary Mirror", *Iraqi Journal of Science*, vol. 64, no. 12, pp. 6638- 6647, 2023. DOI: 10.24996/ijs.2023.64.12.42

[2] F. OLIVER, and J. DASHWOOD, "Characterisation of Tomographic Adaptive Optics Performance in Realistic Atmospheric Conditions," *Doctoral thesis, Durham University*, Durham, UK, 2020.

[3] A. Ayet, and B. Chapron, "The Dynamical Coupling of Wind-Waves and Atmospheric Turbulence: A Review of Theoretical and Phenomenological Models," *Boundary-Layer Meteorology*, vol. 183, pp. 1–33, 2022. https://doi.org/10.1007/s10546-021-00666-6

[4] R. N. Hassan, and H. Sh. Ali, "Performance Estimation and System Modeling for Refractive Index Structure Constant Cn2", *Karbala International Journal of Modern Science*: vol. 9, Iss. 2, pp. 178-186, 2023. https://doi.org/10.33640/2405-609X.3291

[5] B. R. Hunt, A L. Iler, and D. G. Sheppard, "Local resolution characteristics of atmosphericturbulence", Optics Express 15388,vol. 30, no. 9 / 25, 2022. https://doi.org/10.1364/OE.457417

[6] E. Aristidi, A. Ziad, J. Chab´e, Y. F.Caujolle, C. Renaud and C. Giordano, "A generalized differential image motion monitor," *Monthly Notices of the Royal Astronomical Society*, vol. 486, Issue 1, pp. 915–925, 2019. https://doi.org/10.1093/mnras/stz854

[1] M. Lamb, C. Correia, S. Sivanandam, R. Swanson, and P. Zavyalova, "Simultaneous Estimation Of Segmented Telescope Phasing Errors and Non-Common Path Aberrations From Adaptive Optics Corrected Images", *Monthly Notices of the Royal Astronomical Society*, Vol. 505, Issue 3, Pages 3347–3360, 2021.https://doi.org/10.1093/mnras/stab1247

[7] U.E. Jallod, "Simulations of Four Types of Optical Aberrations using Zernik Polynomials," Iraqi Journal of Science, vol. 58, no. 1C, pp. 583-591, 2017.

[8] M. Xu, S. Sha, Q. Li, G. Sun, Y. Han, and N. Weng, "Optical Turbulence Profile Forecasting and Verification in the Offshore Atmospheric Boundary Layer", *Applied Sciences*, vol.11, Issue. 18, pp. 8523, 2021. https://doi.org/10.3390/app11188523

[9] V. Kornilov, " Stellar scintillation on large and extremely large telescopes**,"** *Monthly Notices of the Royal Astronomical Society*, vol. 426, Issue 1, pp. 647–655, 2012. https://doi.org/10.1111/j.1365-2966.2012.21653.x

[10] J. Hellemeier, R. Yang, M. Sarazin, and P. Hickson, "Weather at selected astronomical sites-An overview of five atmospheric parameters", *Monthly Notices of the Royal Astronomical Society*, vol.482, Issue 4, pp.4941–4950, 2019. https://doi.org/10.1093/mnras/sty2982.

[11] I. A. Rosu, M. M. Cazacu, O. S. Prelipceanu, and M. Agop, "A Turbulence-Oriented Approach to Retrieve Various Atmospheric Parameters Using Advanced Lidar Data Processing Techniques," *Atmosphere*, vol. 10, no. 38, 2019, doi:10.3390/atmos10010038

[12] A. Otarola, C. De Breuck, T. Travouillon, S. Matsushita, L.-Å. Nyman, A. Wootten, S. Radford, M. Sarazin, F. Kerber, and J. Pérez-Beaupuits, "Precipitable Water Vapor, Temperature, and Wind Statistics at Sites Suitable for mm and Submm Wavelength, Astronomy in Northern Chile," *Publications of the Astronomical Society of the Pacific*, vol.131, no. 988, pp.045001, 2019. https://doi.org/10.1088/1538-3873/aafb78

[13] D. Dravins, L. Lindegren, E. Mezey and A. T. Young, "Atmospheric Intensity Scintillation of Stars. I. Statistical Distributions and Temporal Properties", *Publications of the Astronomical Society of the Pacific*, vol. 109, no. 732, pp.173-207, 1997. https://www.jstor.org/stable/40680883

[14] F. Quatresooz, D. Vanhoenacker-Janvier, and C. Oestges, "Computation of Optical Refractive Index Structure Parameter from its Statistical Definition Using Radiosonde Data," *Radio Science*, vol. 58, Issue 1, pp. 7624, 2023. https://doi.org/10.1029/2022RS007624

[15] S. Wu, X. Wu, C. Su, Q. Yang, J. Xu, T. Luo, and C. Huang, C. Qing, "Reliable model to estimate the profile of the refractive index structure parameter (Cn2) and integrated astroclimatic

parameters in the atmosphere", *Optics Express*, vol. 29, no. 8, pp.12454-12470, 2021. https://doi.org/10.1364/OE.419823

[16] H. Sh. Ali, "Performance Estimation of Solar Imagery Using Different Types of Atmospheric Turbulence Models," *Iraqi Journal of Science*, vol.64, Issue 7, pp: 4579-4590, 2023.

[17] Z. Cheng, L. He, C. Mu, X. Zhang, X. Jing, and J. Zhu, "Inversion of atmospheric turbulence profiles based on generalized Hufnagel-Valley model and DCIM lidar," *Proceeding of SPIE,* vol.12057, pp.120573V, 2021. https://doi.org/10.1117/12.2606700

[18] L. B. Stotts, And L. C. Andrews, "Improving the Hufnagel-Andrews-Phillips refractive index structure parameter model using turbulent intensity," ***Optics Express,*** vol. 31, Issue 9, pp. 14265-14277, 2023. https://doi.org/10.1364/OE.488544

[19] https://weather.uwyo.edu/upperair/bufrraob.shtml